ADJOINT-BASED OPTIMIZATION AND INVERSE DESIGN OF PHOTONIC DEVICES

A DISSERTATION
SUBMITTED TO THE DEPARTMENT OF APPLIED PHYSICS
AND THE COMMITTEE ON GRADUATE STUDIES
OF STANFORD UNIVERSITY
IN PARTIAL FULFILLMENT OF THE REQUIREMENTS
FOR THE DEGREE OF
DOCTOR OF PHILOSOPHY

Tyler William Hughes
June 2019

I certify that I have read this dissertation and that, in my opinion, it is fully adequate in scope and quality as a dissertation for the degree of Doctor of Philosophy.

(Shanhui Fan) Principal Adviser

I certify that I have read this dissertation and that, in my opinion, it is fully adequate in scope and quality as a dissertation for the degree of Doctor of Philosophy.

(Robert L. Byer)

I certify that I have read this dissertation and that, in my opinion, it is fully adequate in scope and quality as a dissertation for the degree of Doctor of Philosophy.

(Olav Solgaard)

I certify that I have read this dissertation and that, in my opinion, it is fully adequate in scope and quality as a dissertation for the degree of Doctor of Philosophy.

(Mark Brongersma)

I certify that I have read this dissertation and that, in my opinion, it is fully adequate in scope and quality as a dissertation for the degree of Doctor of Philosophy.

(Amir Safavi-Naeini)

Approved for the Stanford University Committee on Graduate Studies

Preface

This thesis tells you everything you need to know about...

Acknowledgments

I would like to thank ...

Contents

List of Tables

List of Figures

Chapter 1

Introduction

1.1 Photonics

The field of photonics is concerned with the study and manipulation of light. This endeavor has given rise to countless technologies of great practical and scientific interest. Most prominently, the use of light as an information carrier has enabled high speed and low loss communications through the use of optical fiber technologies [1]. Light is also used extensively for precise detection and measurement in scientific studies. For example, X-ray radiation is now used to observe femtosecond dynamics in chemical reactions [4], and laser interferometry was recently used to measure gravitational waves emitted from black hole mergers [5]. Apart from these, there are many applications of photonics with significant practical importance ranging from renewable energy [2, 7] to heat transfer [6, 3].

One of the most important achievements of photonics in the past few decades has been the development of *integrated* photonic devices [integrated]. In this paradigm, rather than constructing devices using macroscopic components, such as lenses and mirrors, they are created on the surface of a chip using techniques common to the semiconductor industry. Such an approach is appealing as it allows for compact, low cost, and highly functional devices that are also easier to integrate with existing electronic platforms based on composite metal on semiconductor (CMOS) technology [CMOS]. The field of 'Silicon photonics' has especially generated much interest in recent years, in which photonic devices integrated on Silicon are employed in applications ranging from optical interconnects for fast data transfer between microchips to large scale integrated photonic circuits [cite Si Pho].

Here, we will primarily explore two emerging technologies based on integrated photonics, (1) Laser-driven particle accelerators on a chip, and (2) optical hardware for machine learning applications. The approach to laser-driven particle acceleration examined here is referred to as 'dielectric laser acceleration', in which charged particles are accelerated by the near field of a patterned dielectric structure driven by an external laser. As we will show, this technology may benefit greatly from

the use of integrated photonic platforms for its eventual practical applications. Integrated photonics is also a promising candidate for building hardware platforms specialized on machine learning tasks. As the transmission of an image through an optical lens passively performs a Fourier transform, reconfigurable integrated photonic devices are capable of performing arbitrary linear operations through pure transmission of optical signals through their domain. As machine learning models are often dominated by linear operations, this technology may provide a platform with higher processing speed, lower energy usage when compared to conventional digital electronics.

1.2 Designing of Photonic Devices

1.2.1 Traditional Design Approach

In any of these applications, the design of the photonic device is of critical importance. The typical approach to such a process is to use physical intuition to propose an initial structure. This structure may be parameterized by several *design variables*, such as geometric or material parameters. These parameters may then optimized, using numerical simulation or experiment, until convergence on a functioning device that further satisfies fabrication constraints, such as minimum feature size, for example. As an example, if one is interested in designing a device routes input light to different ports for different input wavelengths, one such approach would be to combine several wavelength filters into one device and tune their parameters until the functionality is achieved. Such an approach, while intuitive, has a number of potential drawbacks. First, it is dependent on the designer having significant physical intuition about the problem, which is not always available especially in novel applications. Second, the method of tuning parameters by hand is tedious and the time needed to complete such a task generally scales exponentially with the number of design variables. This fact means that the designer is practically limited to examining a small number of design variables or only a few select combinations. The use of few design variables further limits the designer to consider devices within a fixed parameterization. For example, if one were to designing a device for tailored diffraction or transmission characteristics, he or she may decide to explore grating structures parameterized by tooth height, width, and duty cycle, while ignoring other possible designs.

1.2.2 Inverse Design Approach

Inverse design is a radically different approach that has become popularized in photonics within the past decade [inv des]. In this scheme, the overall performance of the device is defined mathematically through an *objective function*, which is then either maximized or minimized using computational and mathematical optimization techniques. This approach allows for automated design of photonic devices that are often more compact and higher performance than their traditionally designed alternatives. Furthermore, this approach allows one to search through a much larger parameter space,

typically on the order of thousands to millions of design variables, which allows the design algorithms to often find structures with complexities often extending beyond the intuition of the designer.

The use of inverse design has a long history in other fields, such as mechanics [mech], aerodynamics [aero], and heat transfer [heat]. However, in the past decade, it has been applied successfully to many photonics problems. A few early examples include the use of inverse design to engineer wavelength splitters [WDM], perfect 90 degree bends in dielectric waveguides [90 Deg], or the design of photonic crystals [PhC]. More recently, it was applied to engineer more exotic phenomena, such as the photonic crystal band structure [PhC band], nonlinear optical responses [nonlin Zin], and metasurfaces [meta]. For a thorough overview of the progress of inverse design in photonics at the time of publishing, we refer the reader to Ref. [A-Rod].

1.3 Introduction to Adjoint Method

As we will explore in detail, the ability to perform inverse design is largely enabled by the ability to efficiently search such a large parameter space. Typically, this is performed using *gradient-based optimization* techniques, which use local gradient information to iteratively progress through the design space. In design problems with several degrees of freedom, gradient-based methods typically converge on local minima much faster than more general optimization techniques such as particle swarm optimization or genetic algorithms [cite], which don't typically use local gradient information.

In problems constrained by physics described by linear systems or differential equations, the *adjoint method* is used to compute these gradients. The adjoint method allows one to compute gradients of the objective function with respect to each of the design parameters in a complexity that is (in practice) independent on the size of the design space. As such, it is the cornerstone of the inverse design works in photonics and other fields.

Here we give a brief introduction to the mathematics behind the adjoint method. Many engineering systems can be described by a linear system of equations $A(\phi)\mathbf{x} = \mathbf{b}$, where A is a sparse matrix that depends on a set of parameters describing the system, ϕ. Solving this equation with source $\mathbf{b}$ results in the solution $\mathbf{x}$, from which an objective function $J = J(\mathbf{x})$ can be computed.

The optimization of this system corresponds to maximizing or minimizing J with respect to the set of parameters ϕ. For this purpose, the adjoint method allows one to calculate the gradient of the objective function $\nabla_\phi J$ for an arbitrary number of parameters. Crucially, this gradient may be obtained with the computational cost of solving only one additional linear system $\hat{A}^T\bar{\mathbf{x}} = -\frac{\partial J}{\partial \mathbf{x}}^T$, which is often called the 'adjoint' problem.

As we will show, this method may be readily applied to the inverse design of electromagnetic devices. In this case, A represents Maxwell's equations describing the device, $\mathbf{x}$ are the electromagnetic fields, and $\mathbf{b}$ is the electric current source.

1.4 Thesis Overview

Like inverse design, the adjoint method has been known in the applied math community for quite some time, and has been applied to numerous other fields. Its application to photonics is quite recent, but has had a significant impact. In this thesis, we will discuss the application of the adjoint method to new applications in photonics. We will also introduce extensions to the adjoint method, which allow it to be applied to new systems and implemented experimentally. The thesis is organized as follows In Chapter 2, we will introduce the mathematical details behind adjoint-based optimization. To give a concrete example, we will focus on its application to laser-driven particle accelerators on a chip. To continue this discussion, in Chapter 3, we will discuss the scaling of laser-driven particle accelerators to longer length scales using photonic integrated circuits. This discussion will motivate the need to use inverse design for new components, and we will discuss efforts to use such techniques to build these systems experimentally. In Chapter 4, we will discuss optical hardware platforms for machine learning applications. The adjoint method will be explored in the context of training an optical neural network, and we will show that its implementation corresponds to the backpropagation algorithm of conventional neural networks. A novel method for experimentally measuring the gradients obtained through the adjoint method will be introduced in the context of machine learning hardware and we will also discuss our exploration of nonlinear optical activation functions and time-domain machine learning processing using wave physics. In Chapter 5, we will explore the extension of the adjoint method to new scenarios in photonics, namely nonlinear and periodically modulated systems. We will conclude in Chapter 6.

Chapter 2

Adjoint-Based Optimization of Accelerator on a Chip

2.1 Conventional Particle Accelerators

2.2 Dielectric Laser Acceleration

Dielectric laser accelerators (DLAs) are periodic dielectric structures that, when illuminated by laser light, create a near-field that may accelerate electrically charged particles such as electrons [england2014dielectric]. A principal figure of merit for these DLA structures is the acceleration gradient, which signifies the amount of energy gain per unit length achieved by a particle that is phased correctly with the driving field. DLAs may sustain acceleration gradients on the order of $\sim$GV m^{-1} when operating using the high peak electric fields supplied by ultrafast (femtosecond) lasers. These acceleration gradients are several orders of magnitude higher than conventional particle accelerators. As a result, the development of DLA can lead to compact particle accelerators that enable new applications.

DLAs take advantage of the fact that dielectric materials have high damage thresholds at short pulse durations and infrared wavelengths [**?**, **?**, **?**] when compared to metal surfaces at microwave frequencies. This allows DLAs to sustain peak electromagnetic fields, and therefore acceleration gradients, that are 1 to 2 orders of magnitude higher than those found in conventional radio frequency (RF) accelerators. Experimental demonstrations of these acceleration gradients have been made practical in recent years by the availability of robust nanofabrication techniques combined with modern solid state laser systems [**?**]. By providing the potential for generating relativistic electron beams in relatively short length scales, DLA technology is projected to have numerous applications

where tabletop accelerators may be useful, including medical imaging, radiation therapy, and X-ray generation [?, ?]. To achieve high energy gain in a compact size, it is of principle interest to design structures that may produce the largest acceleration gradients possible without exceeding their respective damage thresholds.

Several recently demonstrated candidate DLA structures consist of a planar dielectric structure that is periodic along the particle axis with either an semi-open geometry or a narrow (micron to sub-micron) vacuum gap in which the particles travel [?, ?, ?, ?, ?, ?, ?, ?]. These structures are then side-illuminated by laser pulses. Fig. ?? shows a schematic of the setup, with a laser pulse incident from the bottom.

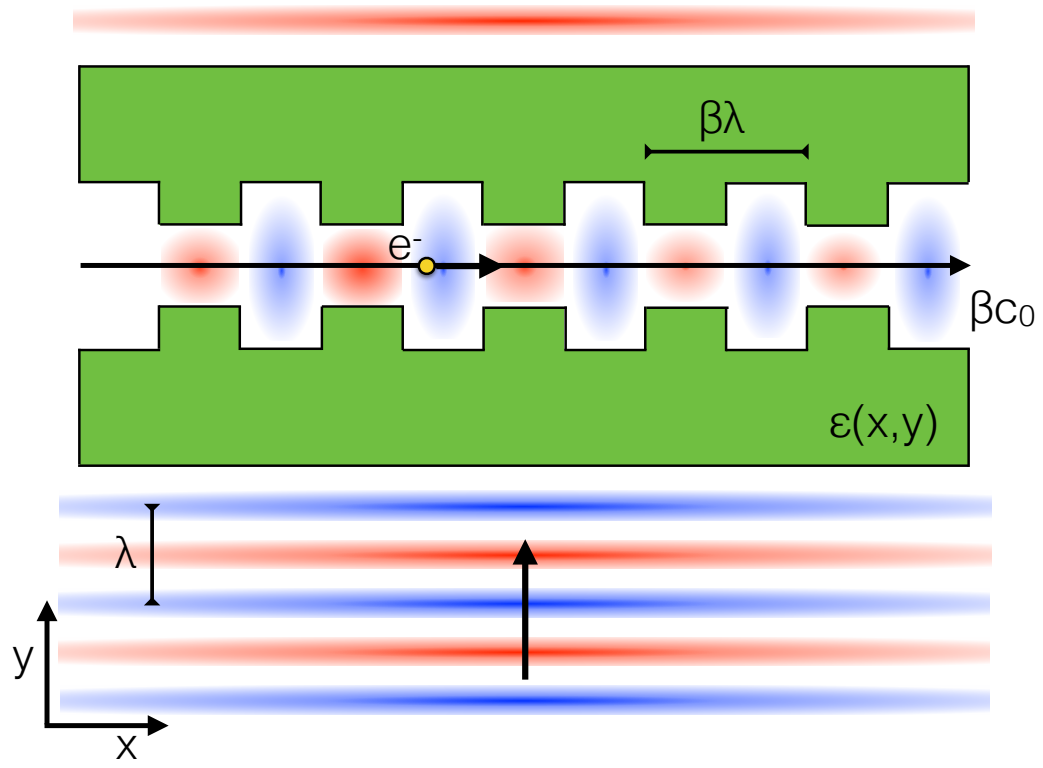

Figure 2.1: Diagram outlining the system setup for side-coupled DLA with an arbitrary dielectric structure $\epsilon(x, y)$ (green). A charged particle moves through the vacuum gap with speed βc_0. The periodicity is set at $\beta\lambda$ where λ is the central wavelength of the laser pulse.

The laser field may also be treated with a pulse front tilt [?, ?] to enable group velocity matching over a distance greater than the laser's pulse length. For acceleration to occur, the dielectric structure must be designed such that the particle feels an electric field that is largely parallel to its

trajectory over many optical periods. In the following calculations, the geometry of the dielectric structure is represented by a spatially varying dielectric constant $\epsilon(x, y)$. We assume invariance in one coordinate ($\hat{z}$) in keeping with the planar symmetry of most current designs. However the methodology we present can be extended to include a third dimension. In addition, our work approximates the incident laser pulse as a monochromatic plane wave at the central frequency, which is a valid approximation as long as the pulse duration is large compared to the optical period.

2.2.1 ACHIP Collaboration

2.2.2 Experimental Demonstrations

2.3 Design of Dielectric Laser Accelerator

2.3.1 Mathematical Definition

In a general DLA system, we may define the acceleration gradient 'G' over a time period 'T' mathematically as follows:

$$G = \frac{1}{T}\int_0^T E_{||}(\vec{r}(t), t)\ dt, \tag{2.1}$$

where $\vec{r}(t)$ is the position of the electron and $E_{||}$ signifies the (real) electric field component parallel to the electron trajectory at a given time.

Since the structure is invariant in the $\hat{z}$ direction, we work in two dimensions, examining only the H_z, E_x and E_y field components. For an approximately monochromatic input laser source with angular frequency ω, the electric fields are, in general, of the form

$$\mathbf{x}(\vec{r}, t) = \Re\left\{\mathbf{x}(\vec{r})e^{i\omega t}\right\}, \tag{2.2}$$

where now $\mathbf{x}$ is complex.

Let us assume the particle we wish to accelerate is moving on the line $y = 0$ with velocity $\vec{v} = \beta c_0 \hat{x}$, where c_0 is the speed of light in vacuum and $\beta \leq 1$. The x position of the particle as a function of time is given by $x(t) = x_0 + \beta c_0 t$, where x_0 represents an arbitrary choice of initial starting position. For normal incidence of the laser (laser propagating in the $+\hat{y}$ direction), phase velocity matching between the particle and the electromagnetic fields is established by introducing a spatial periodicity in our structure of period $\beta\lambda$ along $\hat{x}$, where λ is the laser wavelength. In the limit of an infinitely long structure (or equivalently, $T \to \infty$) we may rewrite our expression for the gradient in Eq. (2.1) as an integral over one spatial period, given by

$$G = \frac{1}{\beta\lambda}\Re\left\{e^{-i\phi_0}\int_0^{\beta\lambda} dx\ E_x(x, 0)e^{i\frac{2\pi}{\beta\lambda}x}\right\}. \tag{2.3}$$

Here the quantity $\phi_0 = \frac{2\pi x_0}{\beta\lambda}$ is representative of the phase of the particle as it enters the spatial period. In further calculations, we set $\phi_0 = 0$, only examining the acceleration gradients experienced by particles entering the accelerator with this specific phase. Since we have arbitrarily control over our input laser phase, this does not impose any constraint on the acceleration gradient attainable.

To simplify the following derivations, we define the following inner product operation involving the integral over two vector quantities $\vec{a}$ and $\vec{b}$ over a single period volume V'

$$\langle \vec{a}, \vec{b} \rangle = \int_{V'} dv \ \left(\vec{a} \cdot \vec{b} \right) = \int_0^{\beta\lambda} dx \int_{-\infty}^{\infty} dy \left(\vec{a} \cdot \vec{b} \right). \tag{2.4}$$

With this definition, we then have the gradient

$$G = \Re \left\{ \langle \vec{E}, \vec{\eta} \rangle \right\}, \tag{2.5}$$

where

$$\vec{\eta}(x, y) = \frac{1}{\beta\lambda} e^{i\frac{2\pi}{\beta\lambda}x} \delta(y)\hat{x}. \tag{2.6}$$

Our goal in designing the accelerator is thus to create a permittivity distribution that maximizes G subject to a few constraints. First, we require that a small gap exist for the electron to travel through the structure. Secondly, we assume that the structure has a finite extent along the direction of the incoming laser beam. We also consider realizing this device through the patterning of a material with permittivity $\epsilon_{\max}$. Therefore, the final device should have permittivity of either 1 or $\epsilon_{\max}$ at all points.

2.3.2 Brute Force Method

To solve such a problem, we may first define a design region in which we allow the permittivity to vary. For the purposes of this example, we consider two slabs surrounding the central accelerator gap, as diagrammed in Fig. [To Do].

We now may consider discretizing our entire spatial domain into a rectangular grid, which will be necessary for numerical simulation. This also allows us to define our design parameters as the permittivity of each grid cell within the design region. Thus, the goal is to find the permittivity of each pixel that will maximize the acceleration gradient, subject to each grid cell having a permittivity value of either 1 or $\epsilon_{\max}$.

To accomplish this, the simplest approach would involve doing a direct search over the full design space. For example, one could label each cell within the design region with an identifier '0' or '1' corresponding to 'vaccuum' and 'material', respectively. Then, one may generate all possible structures and check their respective acceleration gradients.

However, as one can imagine, this method would be far too computationally expensive to perform in practice. For example, even considering a very small design region consisting of $10 \times 10 = 100$

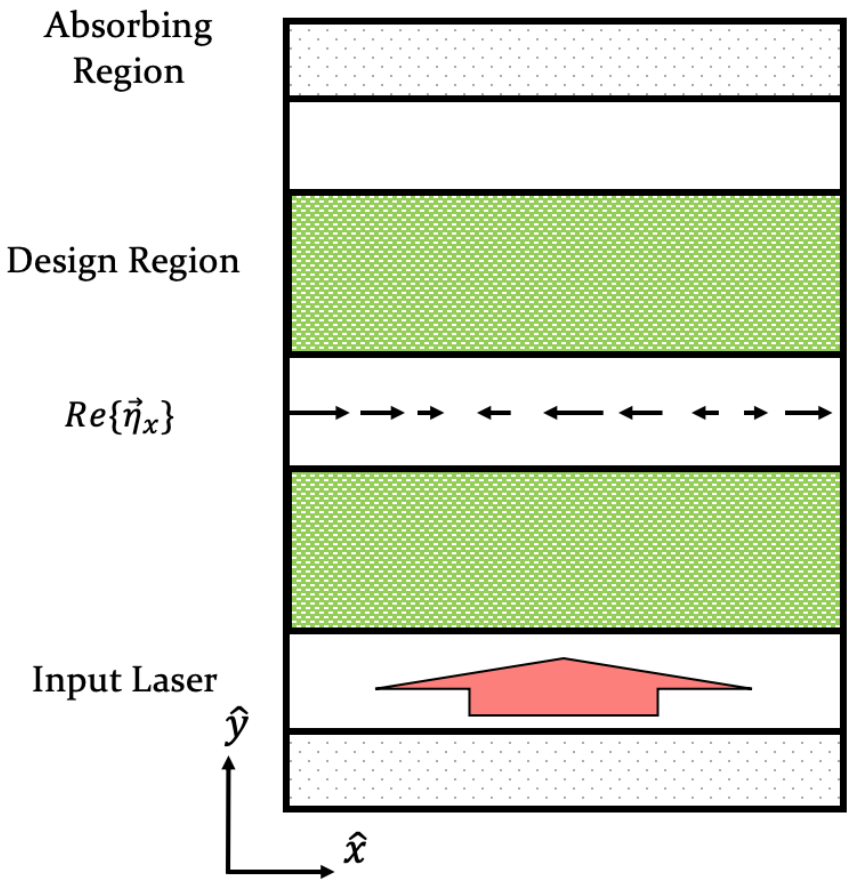

Figure 2.2: Defining Eta

grid cells would result in $2^{100} \approx 10^{30}$ devices to simulate. While one may consider smart ways of searching through this device space without checking each structure, using global optimization approaches such as genetic algorithms [memetic] or particle swarm optimization [particle swarm], this problem is still quite computationally expensive and is exponentially worse as the number of design parameters are increased.

2.3.3 Gradient-based Optimization

A smarter approach involves *gradient-based optimization*, in which we search the design space according to the local gradient of the figure of merit with respect to each of the parameters. For example, we may start with an initially random device, compute how the performance will change with respect to a change in the permittivity of each cell in the design region, and make a small update. This process may be repeated until convergence on a locally optimal solution. If the design

space contains several local optima, then this whole process may be repeated several times with different initial conditions.

In fact, this method is the standard approach to training of neural networks, which may also be framed as an optimization problem over thousands to millions of parameters. We will revisit this connection in a later chapter. While the performance of gradient-based optimization is hard to directly compare to that of global optimization approaches, as the number of design parameters increases, gradient-based optimization are typically preferred as they require far fewer steps in most problems [cite].

For gradient-based optimization to be useful, one would like an efficient means to compute the gradient of the figure of merit with respect to the design parameters. For neural networks, the gradient is computed analytically and then evaluated using the *backpropagation* algorithm [cite backprop]. For photonic devices, one may perform a similar technique using the adjoint method, which allows one to analytically compute the gradient directly from Maxwell's Equations and evaluate the result with only one additional electromagnetic simulation. This remarkable efficiency is largely responsible for the success of inverse design in photonics.

2.4 Adjoint Method

The adjoint method is typically introduced for linear optical systems, although, as we will show in a later chapter, it may be extended to nonlinear systems without much additional effort. In the frequency domain, Maxwell's equations may be written as

$$\nabla \times \nabla \times \vec{E}(\vec{r}) \; - \; k_0^2 \; \epsilon_r(\vec{r}) \; \vec{E}(\vec{r}) \equiv A\vec{E}(\vec{r}) = -i\mu_0\omega\vec{J}(\vec{r}), \tag{2.7}$$

Here, $\vec{E}(\vec{r})$ and $\vec{J}(\vec{r})$ are the electric field and electric current distributions, respectively. $k_0 = \omega/c_0$, ϵ_r is the relative permittivity and a non-magnetic material is assumed ($\mu = \mu_0$)

More abstractly, we may write Eq. (2.7) as

$$A\mathbf{x} = \mathbf{b}, \tag{2.8}$$

where A is a sparse, complex symmetric matrix that encodes Maxwell's equations on the device. $\mathbf{x}$ is a vector containing the electromagnetic fields at each position in the domain, which are the solution to Eq. (2.8) given the vector $\mathbf{b}$ describing the electric current source distribution in the domain.

Our device is described by a set of design variables ϕ, which influence the system matrix, $A = A(\phi)$. Differentiating Eq. (2.7) with respect to ϕ, and assuming that the current source, $\mathbf{b}$, does not

depend on ϕ, we may recover the change in the solution with respect to the parameters as

$$\frac{d\mathbf{x}}{d\phi} = -A^{-1}\frac{\partial A}{\partial \phi}A^{-1}\mathbf{b} = -A^{-1}\frac{\partial A}{\partial \phi}\mathbf{x} \tag{2.9}$$

Now, we consider differentiating an objective function $J = J(\mathbf{x})$ that depends explicitly on the field solution. By the chain rule, this gives

$$\frac{dJ}{d\phi} = -\Re\left\{\frac{\partial J}{\partial \mathbf{x}}\frac{d\mathbf{x}}{d\phi}\right\} = -\Re\left\{\frac{\partial J}{\partial \mathbf{x}}A^{-1}\frac{\partial A}{\partial \phi}\mathbf{x}\right\} \tag{2.10}$$

To evaluate Eq. (2.10), we define a second simulation with source term $-\frac{\partial J}{\partial \mathbf{x}}^T$,

$$A^T\mathbf{x}_{\mathrm{aj}} = A\mathbf{x}_{\mathrm{aj}} = -\frac{\partial J}{\partial \mathbf{x}}^T, \tag{2.11}$$

then the field solution, $\mathbf{x}_{\mathrm{aj}} = -A^{-1}\frac{\partial J}{\partial \mathbf{x}}^T$, can be easily identified in Eq. (2.10), which gives the expression

$$\frac{dG}{d\phi} = \Re\left\{\mathbf{x}_{\mathrm{aj}}^T\frac{\partial A}{\partial \phi}\mathbf{x}\right\}. \tag{2.12}$$

The only quantity in this expression that depends on the parameter ϕ is $\frac{\partial A}{\partial \phi}$. As we will soon discuss, this quantity will generally be trivial to compute. On the other hand, the full field calculations of $\mathbf{x}$ and $\mathbf{x}_{\mathrm{aj}}$ are computationally expensive, but may be computed once and used for an arbitrarily large set of parameters ϕ_i. This gives the adjoint method significant scaling advantage with respect to traditional direct sensitivity methods, such as finite difference, which require a separate full-field calculation for each parameter being investigated.

2.4.1 Application to Accelerator

2.5 Inverse design of Dielectric Laser Accelerator

2.5.1 Optimization Routine

2.5.2 Results and Comparison to Existing Structures

2.5.3 Interpretation of Adjoint Fields as Radiation

Chapter 3

Integrated Photonic Circuit for Accelerators on a Chip

3.1 Motivation

3.2 On-Chip Laser Coupling Device

3.3 Parameter Study

3.4 Automatic Controlled Power Delivery Systems

3.4.1 Phase Control Mechanism

3.4.2 Power Control Mechanism using Reconfigurable Circuit

Deterministic Tuning Algorithm

Scaling Gains

3.5 Experimental Efforts

3.5.1 Waveguide Damage and Nonlinearity Measurements

3.5.2 Demonstration of Waveguide-Coupled Acceleration

Chapter 4

Training of Optical Neural Networks

4.1 Introduction to Machine Learning

4.1.1 Applications

4.1.2 Hardware Demands

4.2 Linear Nanophotonic Processors

4.3 Optical Neural Networks

4.3.1 Conventional Neural Network

4.3.2 Optical Integration

4.3.3 Training Protocols

Computer Model Training

Brute Force Training

4.4 In Situ Backpropagation Training

4.4.1 Derivation Using Adjoint Method

4.4.2 Method for Measurement of Adjoint Gradient

4.4.3 Numerical Demonstrations

4.5 Electro-Optic Activation Functions

4.5.1 Motivation

Chapter 5

Extension of Adjoint Method beyond Linear Time-Invariant Systems.

5.1 Nonlinear Devices

5.1.1 Generalization of Adjoint Method to Nonlinear Problems

5.1.2 Inverse Design of Nonlinear Photonic Switches

5.2 Active Devices

5.2.1 Adjoint Sensitivity for Multi-Frequency FDFD Problems

5.2.2 Inverse Design of Optical Isolators through Dynamic Modulation

5.3 Adjoint for Time Domain

5.3.1 Derivation

5.3.2 Challenges

5.4 Forward-mode Differentiation

Chapter 6

Conclusion and Final Remarks

Appendix A

Something

Some appendix section.

Bibliography

[1] Govind P. Agrawal. *Fiber-Optic Communication Systems.* John Wiley & Sons, February 2012.

[2] D. E. Carlson and C. R. Wronski. Amorphous silicon solar cell. *Applied Physics Letters*, 28(11):671–673, June 1976.

[3] Po-Chun Hsu, Alex Y. Song, Peter B. Catrysse, Chong Liu, Yucan Peng, Jin Xie, Shanhui Fan, and Yi Cui. Radiative human body cooling by nanoporous polyethylene textile. *Science*, 353(6303):1019–1023, September 2016.

[4] Jan Kern, Ruchira Chatterjee, Iris D. Young, Franklin D. Fuller, Louise Lassalle, Mohamed Ibrahim, Sheraz Gul, Thomas Fransson, Aaron S. Brewster, Roberto Alonso-Mori, Rana Hussein, Miao Zhang, Lacey Douthit, Casper de Lichtenberg, Mun Hon Cheah, Dmitry Shevela, Julia Wersig, Ina Seuffert, Dimosthenis Sokaras, Ernest Pastor, Clemens Weninger, Thomas Kroll, Raymond G. Sierra, Pierre Aller, Agata Butryn, Allen M. Orville, Mengning Liang, Alexander Batyuk, Jason E. Koglin, Sergio Carbajo, Sébastien Boutet, Nigel W. Moriarty, James M. Holton, Holger Dobbek, Paul D. Adams, Uwe Bergmann, Nicholas K. Sauter, Athina Zouni, Johannes Messinger, Junko Yano, and Vittal K. Yachandra. Structures of the intermediates of Kok's photosynthetic water oxidation clock. *Nature*, 563(7731):421, November 2018.

[5] LIGO Scientific Collaboration and Virgo Collaboration, B. P. Abbott, R. Abbott, T. D. Abbott, M. R. Abernathy, F. Acernese, K. Ackley, C. Adams, T. Adams, P. Addesso, R. X. Adhikari, V. B. Adya, C. Affeldt, M. Agathos, K. Agatsuma, N. Aggarwal, O. D. Aguiar, L. Aiello, A. Ain, P. Ajith, B. Allen, A. Allocca, P. A. Altin, S. B. Anderson, W. G. Anderson, K. Arai, M. A. Arain, M. C. Araya, C. C. Arceneaux, J. S. Areeda, N. Arnaud, K. G. Arun, S. Ascenzi, G. Ashton, M. Ast, S. M. Aston, P. Astone, P. Aufmuth, C. Aulbert, S. Babak, P. Bacon, M. K. M. Bader, P. T. Baker, F. Baldaccini, G. Ballardin, S. W. Ballmer, J. C. Barayoga, S. E. Barclay, B. C. Barish, D. Barker, F. Barone, B. Barr, L. Barsotti, M. Barsuglia, D. Barta, J. Bartlett, M. A. Barton, I. Bartos, R. Bassiri, A. Basti, J. C. Batch, C. Baune, V. Bavigadda, M. Bazzan, B. Behnke, M. Bejger, C. Belczynski, A. S. Bell, C. J. Bell, B. K. Berger, J. Bergman, G. Bergmann, C. P. L. Berry, D. Bersanetti, A. Bertolini, J. Betzwieser, S. Bhagwat, R. Bhandare,

I. A. Bilenko, G. Billingsley, J. Birch, R. Birney, O. Birnholtz, S. Biscans, A. Bisht, M. Bitossi, C. Biwer, M. A. Bizouard, J. K. Blackburn, C. D. Blair, D. G. Blair, R. M. Blair, S. Bloemen, O. Bock, T. P. Bodiya, M. Boer, G. Bogaert, C. Bogan, A. Bohe, P. Bojtos, C. Bond, F. Bondu, R. Bonnand, B. A. Boom, R. Bork, V. Boschi, S. Bose, Y. Bouffanais, A. Bozzi, C. Bradaschia, P. R. Brady, V. B. Braginsky, M. Branchesi, J. E. Brau, T. Briant, A. Brillet, M. Brinkmann, V. Brisson, P. Brockill, A. F. Brooks, D. A. Brown, D. D. Brown, N. M. Brown, C. C. Buchanan, A. Buikema, T. Bulik, H. J. Bulten, A. Buonanno, D. Buskulic, C. Buy, R. L. Byer, M. Cabero, L. Cadonati, G. Cagnoli, C. Cahillane, J. Calderón Bustillo, T. Callister, E. Calloni, J. B. Camp, K. C. Cannon, J. Cao, C. D. Capano, E. Capocasa, F. Carbognani, S. Caride, J. Casanueva Diaz, C. Casentini, S. Caudill, M. Cavaglià, F. Cavalier, R. Cavalieri, G. Cella, C. B. Cepeda, L. Cerboni Baiardi, G. Cerretani, E. Cesarini, R. Chakraborty, T. Chalermsongsak, S. J. Chamberlin, M. Chan, S. Chao, P. Charlton, E. Chassande-Mottin, H. Y. Chen, Y. Chen, C. Cheng, A. Chincarini, A. Chiummo, H. S. Cho, M. Cho, J. H. Chow, N. Christensen, Q. Chu, S. Chua, S. Chung, G. Ciani, F. Clara, J. A. Clark, F. Cleva, E. Coccia, P.-F. Cohadon, A. Colla, C. G. Collette, L. Cominsky, M. Constancio, A. Conte, L. Conti, D. Cook, T. R. Corbitt, N. Cornish, A. Corsi, S. Cortese, C. A. Costa, M. W. Coughlin, S. B. Coughlin, J.-P. Coulon, S. T. Countryman, P. Couvares, E. E. Cowan, D. M. Coward, M. J. Cowart, D. C. Coyne, R. Coyne, K. Craig, J. D. E. Creighton, T. D. Creighton, J. Cripe, S. G. Crowder, A. M. Cruise, A. Cumming, L. Cunningham, E. Cuoco, T. Dal Canton, S. L. Danilishin, S. D'Antonio, K. Danzmann, N. S. Darman, C. F. Da Silva Costa, V. Dattilo, I. Dave, H. P. Daveloza, M. Davier, G. S. Davies, E. J. Daw, R. Day, S. De, D. DeBra, G. Debreczeni, J. Degallaix, M. De Laurentis, S. Deléglise, W. Del Pozzo, T. Denker, T. Dent, H. Dereli, V. Dergachev, R. T. DeRosa, R. De Rosa, R. DeSalvo, S. Dhurandhar, M. C. Díaz, L. Di Fiore, M. Di Giovanni, A. Di Lieto, S. Di Pace, I. Di Palma, A. Di Virgilio, G. Dojcinoski, V. Dolique, F. Donovan, K. L. Dooley, S. Doravari, R. Douglas, T. P. Downes, M. Drago, R. W. P. Drever, J. C. Driggers, Z. Du, M. Ducrot, S. E. Dwyer, T. B. Edo, M. C. Edwards, A. Effler, H.-B. Eggenstein, P. Ehrens, J. Eichholz, S. S. Eikenberry, W. Engels, R. C. Essick, T. Etzel, M. Evans, T. M. Evans, R. Everett, M. Factourovich, V. Fafone, H. Fair, S. Fairhurst, X. Fan, Q. Fang, S. Farinon, B. Farr, W. M. Farr, M. Favata, M. Fays, H. Fehrmann, M. M. Fejer, D. Feldbaum, I. Ferrante, E. C. Ferreira, F. Ferrini, F. Fidecaro, L. S. Finn, I. Fiori, D. Fiorucci, R. P. Fisher, R. Flaminio, M. Fletcher, H. Fong, J.-D. Fournier, S. Franco, S. Frasca, F. Frasconi, M. Frede, Z. Frei, A. Freise, R. Frey, V. Frey, T. T. Fricke, P. Fritschel, V. V. Frolov, P. Fulda, M. Fyffe, H. A. G. Gabbard, J. R. Gair, L. Gammaitoni, S. G. Gaonkar, F. Garufi, A. Gatto, G. Gaur, N. Gehrels, G. Gemme, B. Gendre, E. Genin, A. Gennai, J. George, L. Gergely, V. Germain, Abhirup Ghosh, Archisman Ghosh, S. Ghosh, J. A. Giaime, K. D. Giardina, A. Giazotto, K. Gill, A. Glaefke, J. R. Gleason, E. Goetz, R. Goetz, L. Gondan, G. González, J. M. Gonzalez Castro, A. Gopakumar, N. A. Gordon, M. L. Gorodetsky, S. E. Gossan, M. Gosselin, R. Gouaty, C. Graef, P. B. Graff, M. Granata, A. Grant,

S. Gras, C. Gray, G. Greco, A. C. Green, R. J. S. Greenhalgh, P. Groot, H. Grote, S. Grunewald, G. M. Guidi, X. Guo, A. Gupta, M. K. Gupta, K. E. Gushwa, E. K. Gustafson, R. Gustafson, J. J. Hacker, B. R. Hall, E. D. Hall, G. Hammond, M. Haney, M. M. Hanke, J. Hanks, C. Hanna, M. D. Hannam, J. Hanson, T. Hardwick, J. Harms, G. M. Harry, I. W. Harry, M. J. Hart, M. T. Hartman, C.-J. Haster, K. Haughian, J. Healy, J. Heefner, A. Heidmann, M. C. Heintze, G. Heinzel, H. Heitmann, P. Hello, G. Hemming, M. Hendry, I. S. Heng, J. Hennig, A. W. Heptonstall, M. Heurs, S. Hild, D. Hoak, K. A. Hodge, D. Hofman, S. E. Hollitt, K. Holt, D. E. Holz, P. Hopkins, D. J. Hosken, J. Hough, E. A. Houston, E. J. Howell, Y. M. Hu, S. Huang, E. A. Huerta, D. Huet, B. Hughey, S. Husa, S. H. Huttner, T. Huynh-Dinh, A. Idrisy, N. Indik, D. R. Ingram, R. Inta, H. N. Isa, J.-M. Isac, M. Isi, G. Islas, T. Isogai, B. R. Iyer, K. Izumi, M. B. Jacobson, T. Jacqmin, H. Jang, K. Jani, P. Jaranowski, S. Jawahar, F. Jiménez-Forteza, W. W. Johnson, N. K. Johnson-McDaniel, D. I. Jones, R. Jones, R. J. G. Jonker, L. Ju, K. Haris, C. V. Kalaghatgi, V. Kalogera, S. Kandhasamy, G. Kang, J. B. Kanner, S. Karki, M. Kasprzack, E. Katsavounidis, W. Katzman, S. Kaufer, T. Kaur, K. Kawabe, F. Kawazoe, F. Kéfélian, M. S. Kehl, D. Keitel, D. B. Kelley, W. Kells, R. Kennedy, D. G. Keppel, J. S. Key, A. Khalaidovski, F. Y. Khalili, I. Khan, S. Khan, Z. Khan, E. A. Khazanov, N. Kijbunchoo, C. Kim, J. Kim, K. Kim, Nam-Gyu Kim, Namjun Kim, Y.-M. Kim, E. J. King, P. J. King, D. L. Kinzel, J. S. Kissel, L. Kleybolte, S. Klimenko, S. M. Koehlenbeck, K. Kokeyama, S. Koley, V. Kondrashov, A. Kontos, S. Koranda, M. Korobko, W. Z. Korth, I. Kowalska, D. B. Kozak, V. Kringel, B. Krishnan, A. Królak, C. Krueger, G. Kuehn, P. Kumar, R. Kumar, L. Kuo, A. Kutynia, P. Kwee, B. D. Lackey, M. Landry, J. Lange, B. Lantz, P. D. Lasky, A. Lazzarini, C. Lazzaro, P. Leaci, S. Leavey, E. O. Lebigot, C. H. Lee, H. K. Lee, H. M. Lee, K. Lee, A. Lenon, M. Leonardi, J. R. Leong, N. Leroy, N. Letendre, Y. Levin, B. M. Levine, T. G. F. Li, A. Libson, T. B. Littenberg, N. A. Lockerbie, J. Logue, A. L. Lombardi, L. T. London, J. E. Lord, M. Lorenzini, V. Loriette, M. Lormand, G. Losurdo, J. D. Lough, C. O. Lousto, G. Lovelace, H. Lück, A. P. Lundgren, J. Luo, R. Lynch, Y. Ma, T. MacDonald, B. Machenschalk, M. MacInnis, D. M. Macleod, F. Magaña-Sandoval, R. M. Magee, M. Mageswaran, E. Majorana, I. Maksimovic, V. Malvezzi, N. Man, I. Mandel, V. Mandic, V. Mangano, G. L. Mansell, M. Manske, M. Mantovani, F. Marchesoni, F. Marion, S. Márka, Z. Márka, A. S. Markosyan, E. Maros, F. Martelli, L. Martellini, I. W. Martin, R. M. Martin, D. V. Martynov, J. N. Marx, K. Mason, A. Masserot, T. J. Massinger, M. Masso-Reid, F. Matichard, L. Matone, N. Mavalvala, N. Mazumder, G. Mazzolo, R. McCarthy, D. E. McClelland, S. McCormick, S. C. McGuire, G. McIntyre, J. McIver, D. J. McManus, S. T. McWilliams, D. Meacher, G. D. Meadors, J. Meidam, A. Melatos, G. Mendell, D. Mendoza-Gandara, R. A. Mercer, E. Merilh, M. Merzougui, S. Meshkov, C. Messenger, C. Messick, P. M. Meyers, F. Mezzani, H. Miao, C. Michel, H. Middleton, E. E. Mikhailov, L. Milano, J. Miller, M. Millhouse, Y. Minenkov, J. Ming, S. Mirshekari, C. Mishra, S. Mitra, V. P. Mitrofanov, G. Mitselmakher, R. Mittleman, A. Moggi, M. Mohan, S. R. P. Mohapatra, M. Montani, B. C.

Moore, C. J. Moore, D. Moraru, G. Moreno, S. R. Morriss, K. Mossavi, B. Mours, C. M. Mow-Lowry, C. L. Mueller, G. Mueller, A. W. Muir, Arunava Mukherjee, D. Mukherjee, S. Mukherjee, N. Mukund, A. Mullavey, J. Munch, D. J. Murphy, P. G. Murray, A. Mytidis, I. Nardecchia, L. Naticchioni, R. K. Nayak, V. Necula, K. Nedkova, G. Nelemans, M. Neri, A. Neunzert, G. Newton, T. T. Nguyen, A. B. Nielsen, S. Nissanke, A. Nitz, F. Nocera, D. Nolting, M. E. N. Normandin, L. K. Nuttall, J. Oberling, E. Ochsner, J. O'Dell, E. Oelker, G. H. Ogin, J. J. Oh, S. H. Oh, F. Ohme, M. Oliver, P. Oppermann, Richard J. Oram, B. O'Reilly, R. O'Shaughnessy, C. D. Ott, D. J. Ottaway, R. S. Ottens, H. Overmier, B. J. Owen, A. Pai, S. A. Pai, J. R. Palamos, O. Palashov, C. Palomba, A. Pal-Singh, H. Pan, Y. Pan, C. Pankow, F. Pannarale, B. C. Pant, F. Paoletti, A. Paoli, M. A. Papa, H. R. Paris, W. Parker, D. Pascucci, A. Pasqualetti, R. Passaquieti, D. Passuello, B. Patricelli, Z. Patrick, B. L. Pearlstone, M. Pedraza, R. Pedurand, L. Pekowsky, A. Pele, S. Penn, A. Perreca, H. P. Pfeiffer, M. Phelps, O. Piccinni, M. Pichot, M. Pickenpack, F. Piergiovanni, V. Pierro, G. Pillant, L. Pinard, I. M. Pinto, M. Pitkin, J. H. Poeld, R. Poggiani, P. Popolizio, A. Post, J. Powell, J. Prasad, V. Predoi, S. S. Premachandra, T. Prestegard, L. R. Price, M. Prijatelj, M. Principe, S. Privitera, R. Prix, G. A. Prodi, L. Prokhorov, O. Puncken, M. Punturo, P. Puppo, M. Pürrer, H. Qi, J. Qin, V. Quetschke, E. A. Quintero, R. Quitzow-James, F. J. Raab, D. S. Rabeling, H. Radkins, P. Raffai, S. Raja, M. Rakhmanov, C. R. Ramet, P. Rapagnani, V. Raymond, M. Razzano, V. Re, J. Read, C. M. Reed, T. Regimbau, L. Rei, S. Reid, D. H. Reitze, H. Rew, S. D. Reyes, F. Ricci, K. Riles, N. A. Robertson, R. Robie, F. Robinet, A. Rocchi, L. Rolland, J. G. Rollins, V. J. Roma, J. D. Romano, R. Romano, G. Romanov, J. H. Romie, D. Rosińska, S. Rowan, A. Rüdiger, P. Ruggi, K. Ryan, S. Sachdev, T. Sadecki, L. Sadeghian, L. Salconi, M. Saleem, F. Salemi, A. Samajdar, L. Sammut, L. M. Sampson, E. J. Sanchez, V. Sandberg, B. Sandeen, G. H. Sanders, J. R. Sanders, B. Sassolas, B. S. Sathyaprakash, P. R. Saulson, O. Sauter, R. L. Savage, A. Sawadsky, P. Schale, R. Schilling, J. Schmidt, P. Schmidt, R. Schnabel, R. M. S. Schofield, A. Schönbeck, E. Schreiber, D. Schuette, B. F. Schutz, J. Scott, S. M. Scott, D. Sellers, A. S. Sengupta, D. Sentenac, V. Sequino, A. Sergeev, G. Serna, Y. Setyawati, A. Sevigny, D. A. Shaddock, T. Shaffer, S. Shah, M. S. Shahriar, M. Shaltev, Z. Shao, B. Shapiro, P. Shawhan, A. Sheperd, D. H. Shoemaker, D. M. Shoemaker, K. Siellez, X. Siemens, D. Sigg, A. D. Silva, D. Simakov, A. Singer, L. P. Singer, A. Singh, R. Singh, A. Singhal, A. M. Sintes, B. J. J. Slagmolen, J. R. Smith, M. R. Smith, N. D. Smith, R. J. E. Smith, E. J. Son, B. Sorazu, F. Sorrentino, T. Souradeep, A. K. Srivastava, A. Staley, M. Steinke, J. Steinlechner, S. Steinlechner, D. Steinmeyer, B. C. Stephens, S. P. Stevenson, R. Stone, K. A. Strain, N. Straniero, G. Stratta, N. A. Strauss, S. Strigin, R. Sturani, A. L. Stuver, T. Z. Summerscales, L. Sun, P. J. Sutton, B. L. Swinkels, M. J. Szczepańczyk, M. Tacca, D. Talukder, D. B. Tanner, M. Tápai, S. P. Tarabrin, A. Taracchini, R. Taylor, T. Theeg, M. P. Thirugnanasambandam, E. G. Thomas, M. Thomas, P. Thomas, K. A. Thorne, K. S. Thorne, E. Thrane, S. Tiwari, V. Tiwari, K. V. Tokmakov, C. Tomlinson, M. Tonelli, C. V. Torres, C. I.

Torrie, D. Töyrä, F. Travasso, G. Traylor, D. Trifirò, M. C. Tringali, L. Trozzo, M. Tse, M. Turconi, D. Tuyenbayev, D. Ugolini, C. S. Unnikrishnan, A. L. Urban, S. A. Usman, H. Vahlbruch, G. Vajente, G. Valdes, M. Vallisneri, N. van Bakel, M. van Beuzekom, J. F. J. van den Brand, C. Van Den Broeck, D. C. Vander-Hyde, L. van der Schaaf, J. V. van Heijningen, A. A. van Veggel, M. Vardaro, S. Vass, M. Vasúth, R. Vaulin, A. Vecchio, G. Vedovato, J. Veitch, P. J. Veitch, K. Venkateswara, D. Verkindt, F. Vetrano, A. Viceré, S. Vinciguerra, D. J. Vine, J.-Y. Vinet, S. Vitale, T. Vo, H. Vocca, C. Vorvick, D. Voss, W. D. Vousden, S. P. Vyatchanin, A. R. Wade, L. E. Wade, M. Wade, S. J. Waldman, M. Walker, L. Wallace, S. Walsh, G. Wang, H. Wang, M. Wang, X. Wang, Y. Wang, H. Ward, R. L. Ward, J. Warner, M. Was, B. Weaver, L.-W. Wei, M. Weinert, A. J. Weinstein, R. Weiss, T. Welborn, L. Wen, P. Weßels, T. Westphal, K. Wette, J. T. Whelan, S. E. Whitcomb, D. J. White, B. F. Whiting, K. Wiesner, C. Wilkinson, P. A. Willems, L. Williams, R. D. Williams, A. R. Williamson, J. L. Willis, B. Willke, M. H. Wimmer, L. Winkelmann, W. Winkler, C. C. Wipf, A. G. Wiseman, H. Wittel, G. Woan, J. Worden, J. L. Wright, G. Wu, J. Yablon, I. Yakushin, W. Yam, H. Yamamoto, C. C. Yancey, M. J. Yap, H. Yu, M. Yvert, A. Zadrożny, L. Zangrando, M. Zanolin, J.-P. Zendri, M. Zevin, F. Zhang, L. Zhang, M. Zhang, Y. Zhang, C. Zhao, M. Zhou, Z. Zhou, X. J. Zhu, M. E. Zucker, S. E. Zuraw, and J. Zweizig. Observation of Gravitational Waves from a Binary Black Hole Merger. *Physical Review Letters*, 116(6):061102, February 2016.

[6] Aaswath P. Raman, Marc Abou Anoma, Linxiao Zhu, Eden Rephaeli, and Shanhui Fan. Passive radiative cooling below ambient air temperature under direct sunlight. *Nature*, 515(7528):540–544, November 2014.

[7] Zongfu Yu, Aaswath Raman, and Shanhui Fan. Fundamental limit of nanophotonic light trapping in solar cells. *Proceedings of the National Academy of Sciences*, 107(41):17491–17496, October 2010.